

Kinetics and Product of the Gas-phase Reaction of ClO with NO₂

Timothy J. Wallington[†] and Richard A. Cox*

Environmental and Medical Sciences, A.E.R.E., Harwell, Oxfordshire

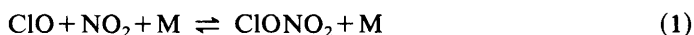
The association reaction of ClO with NO₂ has been studied by infrared absorption spectroscopy and molecular modulation spectroscopy. Photolysis of OClO-NO₂-N₂ mixtures produced ClO radicals over a wide range of reagent concentrations at 303 K, and total pressures of 10 and 25 Torr and 1 atm.† The major product of the association reaction was chlorine nitrate, ClONO₂, with no evidence for the formation of any other isomers.

Observation of the kinetics of OClO removal, ClONO₂ formation and the transient behaviour of ClO are consistent with the following reactions:



The third-order rate coefficient, k_1 , measured from the photolysis of mixtures of [OClO] < 10¹⁴ molecule cm⁻³ was $1.40 \pm 0.07 \times 10^{-31}$ cm⁶ molecule⁻² s⁻¹, in good agreement with previous reports; however, k_1 appeared to decline with increasing OClO concentration. This apparent decline is difficult to rationalize on the basis of existing knowledge.

Chlorine nitrate has been postulated as an important temporary reservoir species¹ in the stratosphere coupling the ClO_x and NO_x catalytic cycles which are responsible for ozone depletion.² Chlorine nitrate is formed by the association reaction of ClO radicals with nitrogen dioxide:



and is removed by photolysis with near-u.v. solar radiation. Although the overall rate constant for the ClO-NO₂ reaction is now rather well known^{3,4} as a result of studies of the rate of loss of ClO in the presence of excess NO₂, there is indirect evidence that other isomers of ClNO₃ may be formed in reaction (1) in addition to the known stable isomer ClONO₂. Thus Knauth⁵ finds a discrepancy between the experimental value of k_1 and the value obtained from measured rates of ClONO₂ decomposition together with the equilibrium constant K_1^* . Molina *et al.*⁶ found apparent discrepancies in both the rate coefficient k_1 and the stoichiometry of reaction (1) when OClO was used as a source of ClO. Theoretical evidence for preferential formation of unstable ClNO₃ isomers in reaction (1) has been proposed.⁷

The formation of isomers in reaction (1) has considerable consequences for stratospheric chemistry since the formation and photolysis of other isomers of ClNO₃ may occur at different rates and by different pathways to those which are believed to apply

[†] Present address: Statewide Air Pollution Research Center, University of California, Riverside, CA 92521, U.S.A.

[‡] 1 Torr ≈ 133.3 Pa; 1 atm = 101 325 Pa.

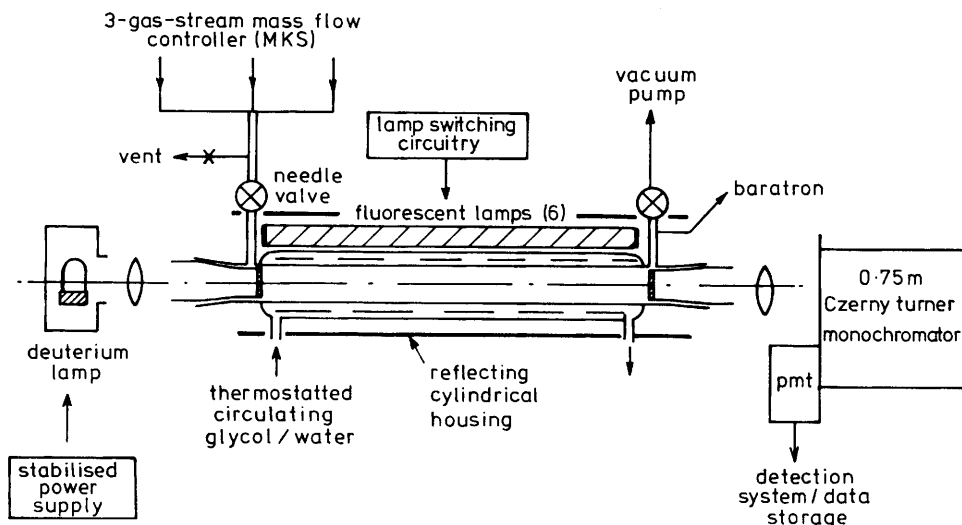
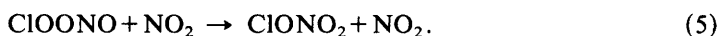


Fig. 1. Schematic diagram of u.v. absorption photochemical spectrometer.

to chlorine nitrate, thereby influencing the temporary reservoir capacity in the coupled ClO_x-NO_x system. Previous work performed in this laboratory,⁸ using i.r. diode laser spectroscopy has shown that the only stable end product of reaction (1) is ClONO₂ and has established the independence of the rate coefficient k_1 with the concentration of NO₂ and Cl₂O over a wide range, thereby precluding the occurrence of isomerization of ClONO₃ species by a chaperon mechanism, *e.g.*



These kinetic measurements were conducted by time-resolved measurements of ClONO₂ and ClO during the photolysis of Cl₂O-NO₂-N₂ mixtures.

Although most of the results concerning the ClO-NO₂ reaction can now be rationalized without postulating isomer formation, the apparent effect of OCIO concentration on the rate coefficient k_1 as determined by Molina *et al.*⁶ in the flash photolysis of OCIO-NO₂ mixtures, is not readily explicable in terms of current knowledge. The main objective of the work reported here was to provide further information on chlorine nitrate formation in systems containing OCIO.

Experimental

Two experimental techniques were employed in the present work. Diode laser spectroscopy was used to identify the product of reaction (1) in the photolysis of gas mixtures containing OCIO and NO₂. The diode laser source spectrometer used (Spectra Physics-Laser Analytics LS3) provided a tunable i.r. source in the region 740-925 cm⁻¹. The 19.8 dm³ photochemical cell consisted of PTFE-coated Pyrex 6 in† pipe section mounted between end plates which supported mirrors in the White optical configuration. The system has been fully described elsewhere.⁸ Molecular modulation spectroscopy, using full-wave analysis, was used for the kinetic studies which employed a smaller cylindrical photochemical quartz cell, 1.2 m long, 1.18 dm³ volume, monitored by a single pass u.v. beam from a well stabilized deuterium lamp. Following dispersion on a monochromator (0.75 m Spex), the monitoring beam was detected using a photomultiplier (EMI 9661).

† 1 in = 2.54 cm.

This apparatus is shown schematically in fig. 1. Subsequent signal processing provided absorption-time profiles during a single photolysis cycle which were stored on a multi-channel analyser as described previously.⁹

Gas flow rates were metered on a mass-flow controller (MKS), and pressures were monitored using an MKS baratron. The photolysis lamps employed in this work were 40 W, 1.2 m fluorescent lamps emitting in a band centred on 420 nm ($380 < \lambda < 480$; Philips 40W/03RS 'Super Actinic'), mounted radially around both reaction cells. For the molecular modulation experiments, the lamps were powered by a special 250 V d.c. square-wave modulated supply.

Materials

Chlorine nitrate was prepared from the reaction of chlorine monoxide (Cl_2O) with nitrogen pentoxide (N_2O_5).¹⁰ These two reagents, which were prepared by standard methods,^{11,12} were condensed in an evacuated glass trap at 77 K (N_2O_5 first, then Cl_2O). The trap was allowed to warm slowly to room temperature. The mixture was distilled several times through a trap at -118°C (ethyl bromide) which retained ClONO_2 . The main impurity was Cl_2 which was slowly removed by repeated fractional distillation. The chlorine nitrate was stored at 196 K at which temperature it was a pale straw-coloured liquid.

Chlorine dioxide was prepared by the action of concentrated sulphuric acid on potassium chlorate. In view of the explosion hazards in preparation and handling OClO , only small amounts were prepared as required. The miniature generator consisted of a 50 cm^3 flask flushed with a flow of dry N_2 connected through a drying tube containing P_2O_5 to a small trap cooled to 196 K. OClO was released immediately when cold concentrated H_2SO_4 was added slowly to KClO_3 crystals (AnalaR grade, B.D.H., 100 mg) in the flask. The yellow gas condensed to an orange solid in the trap.

N_2 (higher purity, B.O.C.) and O_2 (breathing grade, B.O.C.) were taken directly from cylinders. NO_2 from a cylinder (B.D.H., CP grade) was mixed with O_2 (100 Torr) in a 3 dm^3 bulb and left overnight to oxidize any NO to NO_2 . The excess O_2 was then pumped off at 77 K.

Experimental Procedures

Gas mixtures were made up either in the conventional fashion by adding measured partial pressures to the photochemical reactors or in a flowing manifold at atmospheric pressure, from whence a mixture could be pumped through the reaction cell(s) at the required total pressure.

Continuous flowing streams containing constant partial pressures of OClO , NO_2 and ClONO_2 were obtained by passing metered flows of N_2 through traps containing the pure compounds maintained at selected constant temperatures between 196 and 273 K, using appropriate coolant baths. The flows were mixed in a manifold at 1 atm pressure with pure N_2 diluent to obtain the desired concentrations in the cell after pressure reduction over a precision needle valve. Concentrations of species in the reaction cell were measured whenever possible by conventional u.v. absorption using published values for the absorption cross-sections. The values used in this work are summarized in table 1.

I.r. absorption spectra were obtained by scanning the laser frequency slowly through the spectral region of interest, using current tuning of the diode laser. Features on pressure-broadened spectra were enhanced by first derivative detection using a precision lock-in amplifier (Brookdeal model 5903) referenced to a high-frequency (1 kHz) modulation of the diode tuning current. Absolute calibration of frequency required location of absorption due to a known transition in a reference gas; in this case ammonia was used.

Table 1. Absorption cross-sections, σ , employed for concentration measurements

species	λ/nm			
	400	350	277.2	220
	$\sigma/10^{-20} \text{ cm}^2 \text{ molecule}^{-1}$			
Cl ₂ ^a	1.9	18.5	2	—
OCIO ^a	400	1140 (351.5)	43 ^b	—
NO ₂ ^c	67.6	41	4.7	39.6
ClONO ₂ ^c	0.06	0.25	14	344
ClO ^a	—	—	720 ^d	—

^a From ref. (4). ^b Resolution = 0.55 nm. ^c CODATA, ref. (3). ^d Resolution 0.27 nm.

Results

Diode Laser Spectrum of ClONO₂ in the ν_4 Band at 784 cm⁻¹

In the present work, experiments were performed to characterize the ClONO₂ diode laser spectrum in the 784 cm⁻¹ region, so that the products of the ClO-NO₂ reaction would be unequivocally identified from their spectral 'fingerprints' in this region. The results are shown in fig. 2. The diode laser spectrum of ClONO₂ in this region is seen to consist of a crowded and overlapping system of rotational lines. No clear pattern in the rotational lines is discernible. When 10 Torr N₂ was added to the ClONO₂ remaining in the cell after 60 min, spectrum 2(c) was obtained which clearly demonstrates the pressure broadening of the lines and removal of sharp features. Spectrum 2(d) was obtained after the cell had been pumped out and 0.02 Torr NH₃ added. The single line due to NH₃ was assigned as 784.953 cm⁻¹ by reference to the 1980 AFGL trace gas compilation.¹³

For identification and concentration measurement of ClONO₂ formed in the ClO-NO₂ reaction, first-derivative pressure-broadened spectra in the range 784.82-784.88 cm⁻¹ were employed. These spectra are illustrated in fig. 3. Spectrum 3(c) was obtained for pure ClONO₂, whilst spectrum 3(b) shows the same region scanned with the products of photolysis of an OCIO-NO₂ mixture [(9.5 and 2.02) × 10¹⁵ molecule cm⁻³, respectively] in 10 Torr N₂ after 25 s photolysis. The spectra show close similarity, confirming the nature of the product from the ClO-NO₂ reaction, *i.e.* stable ClONO₂.

Quantitative measurements of ClONO₂ production were based on calibration of the peak-to-peak signal in the absorption features marked (A) and (B) on fig. 3, for known amounts of pure ClONO₂ in the cell. From these calibrations the effective differential cross-section for absorption in the 784.829 band [feature (A)] at 10 Torr was *ca.* 2.7 × 10⁻²⁰ cm² molecule⁻¹, giving a minimum detectable concentration of *ca.* 3 × 10¹² molecule cm⁻³ ClONO₂ (100 passes, 0.1% absorption).

When Cl₂O was employed as a source of ClO in a previous study from this laboratory⁹ *via* the reaction:



additional absorptions near the ClONO₂ feature (B) were observed at large extents of reaction of Cl₂O. This was attributed to nitryl chloride, ClNO₂, or its isomer chlorine nitrite, ClONO. In the present study, confirmatory evidence for this species was found in the photolysis of mixtures of Cl₂ and NO₂ (1.2 × 10¹⁶ molecule cm⁻³ each) in 10 Torr N₂. The spectrum fig. 3(a), obtained after photolysis of this mixture, shows bands due

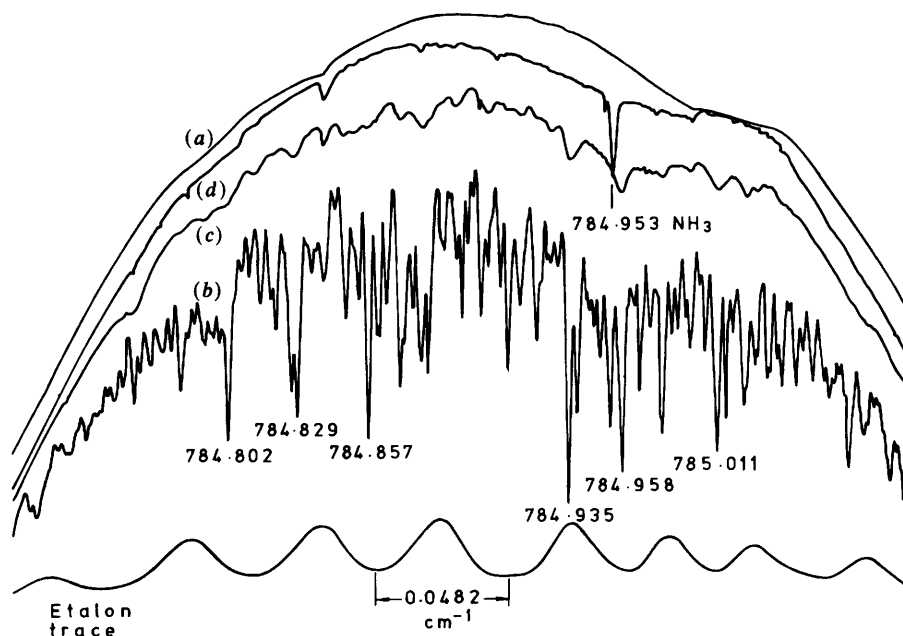


Fig. 2. Diode laser spectra of chlorine nitrate in ν_4 band. Pathlength 2000 cm. (a) Background of source, (b) 0.098 Torr ClONO_2 , (c) ClONO_2 in the presence of 10 Torr N_2 and (d) 0.02 Torr NH_3 . Wavenumbers indicated are relative to the value of 784.953 cm^{-1} assigned to the single NH_3 line recorded.

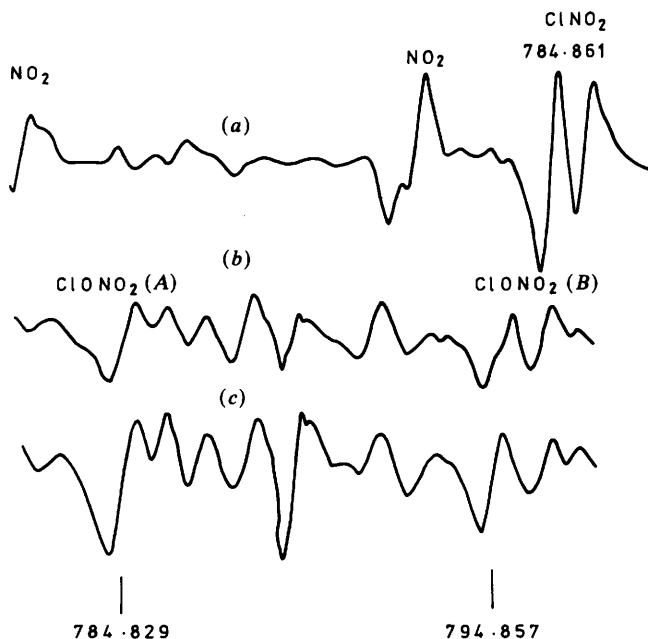


Fig. 3. First derivative, pressure-broadened diode-laser spectra in the 784.8 cm^{-1} region. (a) Products of the photochemical reaction of Cl_2 with NO_2 , (b) photolysis products from photolysis of OClO-NO_2 mixtures and (c) pure ClONO_2 . $l = 3200 \text{ cm}$; $P = 10 \text{ Torr}$, mainly N_2 .

to NO₂ and to a product species which reached a maximum after *ca.* 40 s photolysis and then declined slowly. This behaviour is very similar to that observed by Niki *et al.*¹⁴ in their f.t.i.r. study, where the products of this reaction were shown to be the less stable ClONO isomer (>80% yield) which isomerizes to the more stable ClNO₂. The nearest band centres for ClONO and ClNO₂ are 855.6 cm⁻¹ (Cl—O stretch, argon matrix)¹⁵ and 792.6 cm⁻¹ (N—Cl stretch, gas),¹⁶ therefore the most probable assignment of the line at 784.861 cm⁻¹ is ClNO₂. The apparent steady state of this product can be explained by its formation and removal by the reactions:



Photodissociation Rate of Chlorine Dioxide

In the present work, ClO radicals were generated by photodissociation of chlorine dioxide, OClO, in the reaction



For the determination of product yields from reactions of ClO radicals, it was necessary to measure the rate of reaction (2) as a function of the intensity of the photolysing radiation in the reaction cells. Steady state photolysis of OClO is characterized by autocatalytic behaviour, with acceleration of the rate of consumption of OClO as the reaction proceeds. The determination of the photodissociation rate of OClO can therefore only be achieved by measurement of its decay at very small extents of decomposition of the order of 1%. Furthermore, if O₂ is used as diluent, secondary reactions of O(³P) are avoided since O₃ formation by reaction (9) will be its major fate:



A method was developed for the measurement of small extents of decomposition of OClO using square-wave modulated photolysis pulses of short duration (≤ 0.5 s) on a static mixture, which was replenished for successive experiments. These experiments were conducted in the smaller reaction cell at 303 K and in the presence of 1 atm O₂. Fig. 4 shows the decrease in OClO absorbance at 351.5 nm during a 0.5 s square-wave one-lamp photolysis pulse followed by an equivalent period without illumination. An approximately linear decay of OClO occurs during photolysis, with a small decline during the subsequent dark period. The initial rate of photolysis was obtained from the difference between the mean rates in the light and dark periods. The approximate form of Beer's law for small absorption changes was employed and a photodissociation rate constant, k_a^{OClO} , calculated assuming a quantum yield of one for OClO decay in the presence of O₂,

$$k_a^{\text{OClO}} = -\frac{d(\ln [\text{OClO}])}{dt} = \left(\frac{\Delta I}{I_0}\right) \left(\frac{1}{\Delta t}\right) \quad (i)$$

where $\Delta I/I_0$ is the net decrease in OClO absorption during illumination.

Values of k_a^{OClO} determined in this way for different lamp combinations showed good reproducibility with an average value of $8.6 \times 10^{-3} \text{ s}^{-1}$ per lamp.

The decay of OClO during steady-state photolysis in the presence of NO₂ was also measured. Initial concentrations of OClO and NO₂ were 3.8×10^{14} and 1.1×10^{15} molecule cm⁻³, respectively. In this case, no autocatalytic behaviour was observed, the decline in OClO being strictly logarithmic, as will be seen from the plot in fig. 5.

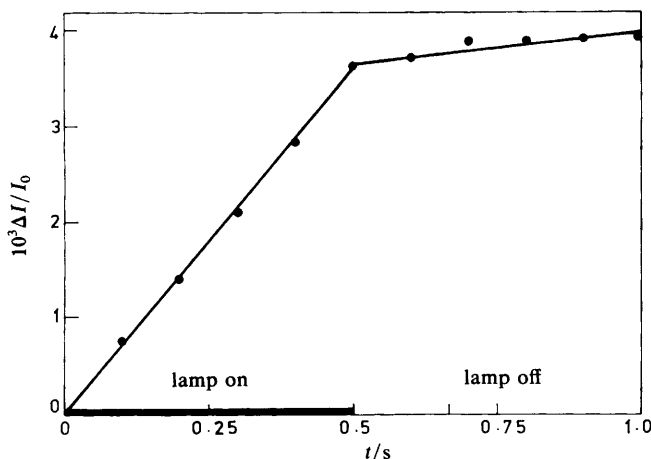
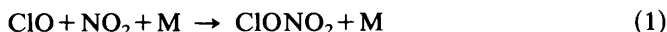
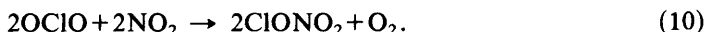


Fig. 4. Decrease in absorption due to OCIO in the static photolysis of OCIO-O₂ mixtures at 1 atm pressure and 303 K. One-lamp photolysis with modulation period $\tau = 1$ s. Initial [OCIO] $\approx 1 \times 10^{15}$ molecule cm⁻³. Data acquired by averaging out several single-shot experiments.

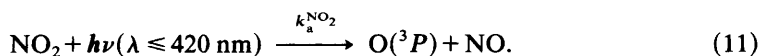
This is consistent with the following mechanism:



which leads to the overall conversion of two molecules of OCIO to chlorine nitrate



The overall decay rate of OCIO was significantly higher than expected from the k_a^{OCIO} measurements. This arises from photodissociation of NO₂ which occurs at a significant rate, particularly when [NO₂] > [OCIO].



Both photofragments lead to production of one molecule of ClO through the above reactions. The photodissociation rate of NO₂, $k_a^{\text{NO}_2}$, was measured in separate experiments in which the decay of NO₂ absorption at 350 nm was measured in steady-state photolysis of 0.6 Torr pure NO₂. The quantum yield for NO₂ photolysis is two under these conditions and analysis of the logarithmic decay plots for different lamp combinations give an average value of $1.9 \times 10^{-3} \text{ s}^{-1}$ per lamp for $k_a^{\text{NO}_2}$. These results allowed the rate of production of ClO radicals during photolysis of OCIO-NO₂ mixtures to be calculated for any lamp combination around the small cell.

For the determination of ClO production rates in the large cell, where ClONO₂ formation was monitored by i.r. absorption, the rate of loss of OCIO was measured simultaneously during the experiments, by absorption at 351.5 or 348 nm. The average value of k_a^{OCIO} in this vessel was $3.5 \times 10^{-3} \text{ s}^{-1}$ for one-lamp photolysis.

Yields for Chlorine Nitrate Formation

The rate of formation of chlorine nitrate in the photolysis of OCIO-NO₂ mixtures was measured using optical absorption for a wide range of reaction conditions. The rates

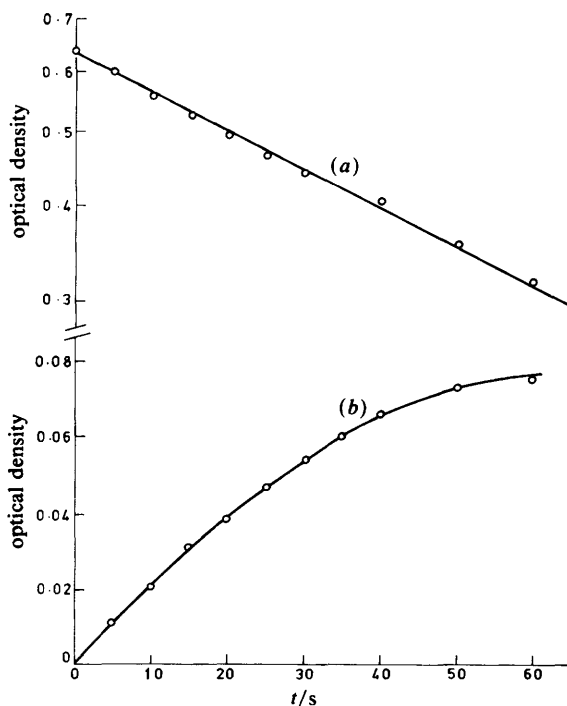
Gas-phase Reaction of ClO with NO₂

Fig. 5. Absorption-time curves for the static photolysis of OClO-NO₂ mixtures in 1 atm N₂, obtained at (a) 351.5 nm (OClO decay) and (b) 220 nm (ClONO₂ formation).

were compared with the rate of photolytic production of ClO and the yield of ClONO₂ from reaction (1) determined from the following relationship

$$\phi(\text{ClONO}_2) = \frac{d[\text{ClONO}_2]/dt}{2k_a^{\text{OClO}}[\text{OClO}] + 2k_a^{\text{NO}_2}[\text{NO}_2]} \quad (\text{ii})$$

the concentrations referring to average values present during the experiment. The rate of OClO removal was also monitored as a check on the ClO production rates and the rate was expressed as a quantum yield according to the following relationship:

$$\phi(\text{OClO}) = \frac{-d[\text{OClO}]/dt}{2k_a^{\text{OClO}}[\text{OClO}] + 2k_a^{\text{NO}_2}[\text{NO}_2]} \quad (\text{iii})$$

Rate measurements using u.v. absorption were conducted in the smaller reaction cell. ClONO₂ formation was monitored at 220 nm and the chlorine nitrate concentration change was determined assuming that optical density changes were due only to ClONO₂ and NO₂ at this wavelength. The small contribution due to absorption by NO₂ was calculated assuming that $\Delta[\text{NO}_2] = \Delta[\text{ClONO}_2]$. OClO was monitored at 351.5 nm except at high [OClO] where the high optical densities dictated use of a less strongly absorbing spectral region at 348 nm. Correction for NO₂ absorption was also required at this wavelength.

The rate measurements were made using both static and flowing mixtures. Fig. 5 shows a typical plot of loss of OClO absorption at 351.5 nm and growth of absorption at 220 nm during steady-state photolysis of a static mixture containing OClO and NO₂ at 1 atm pressure. A linear increase in absorption owing to the formation of ClONO₂ is seen to occur during the initial stages, with a fall off in rate at larger extents of reaction owing to reactant depletion and secondary chemistry.

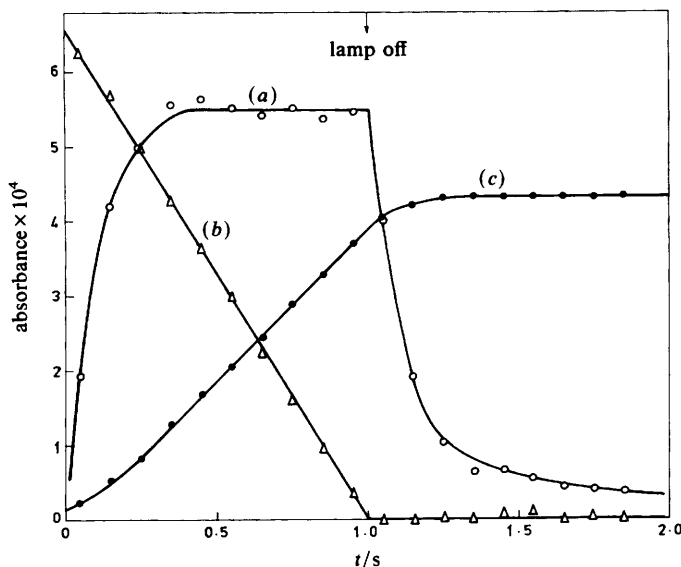


Fig. 6. Time-resolved absorption profiles of OCIO, ClONO₂ and ClO obtained in the 0.5 Hz modulated photolysis of flowing OCIO-NO₂ mixtures at 25.6 Torr total pressure and 303 K one-lamp photolysis. [OCIO]₀ = 2.12 × 10¹⁴ molecule cm⁻³. [NO₂]₀ = 8.0 × 10¹³ molecule cm⁻². (a) ClO, (b) OCIO (absorbance × 10⁻¹) and (c) ClONO₂ (absorbance × 0.2).

In the flow mode, concentration-time changes were monitored during successive modulated photolysis periods applied to the flowing mixture, using the multichannel detector. The signal obtained for stable reactant and product species was a near triangular waveform due to intermittent photochemistry superimposed on a steady-state absorption owing to the balance between flow-in and flow-out of the reaction cell. The effect of flow could be readily subtracted leaving absorption-time curves for a single cycle as illustrated in fig. 6. Rates were determined using the appropriate absorption cross-sections in the usual way, assuming the small absorption approximation for Beer's law. It will be noted on fig. 6 that ClONO₂ formation shows a distinct delay owing to the finite time required for ClO to attain steady state at the modulation period employed. ClONO₂ formation rates were determined from the linear part of the concentration-time curve. OCIO removal did not show a delay since the removal of the OCIO molecule by photolysis plus attack by O or NO occurs on a relatively short time scale. Most of the flow experiments were conducted at a total pressure of 25 Torr. No effect of total pressure on the yields for ClONO₂ formation and OCIO removal, $\phi(\text{ClONO}_2)$, $\phi(\text{OCIO})$, was apparent based on measurements at this pressure and at 1 atm.

Rate measurements of chlorine nitrate formation were also conducted in the larger cell using i.r. absorption in the spectral fingerprint region near 784 cm⁻¹ to determine its concentration. In these experiments, the growth of the differential absorption signals at 784.829 and 784.857 cm⁻¹ was monitored by scanning the spectrum in first-derivative mode after successive 5 or 10 s photolysis periods on a static mixture. Absolute concentrations were then determined from a calibration graph obtained using pure ClONO₂. The decay of OCIO was also monitored in the u.v. and the yield of chlorine nitrate, $\phi(\text{ClONO}_2)$, was determined from the relationship:

$$\phi(\text{ClONO}_2) = \frac{\Delta[\text{ClONO}_2]}{\Delta[\text{OCIO}]} \quad (\text{iv})$$

Gas-phase Reaction of ClO with NO₂**Table 2.** Yield for ClONO₂ formation and OClO removal^a

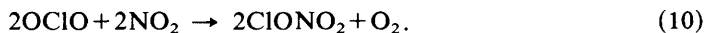
[OClO] /molecule cm ⁻³	number of experiments	$\phi_{av}(\bullet 1\sigma)^b$
chlorine nitrate; u.v.		
<10 ¹⁵	14	1.08 (±0.15)
10 ¹⁵ -10 ¹⁶	9	1.13 (±0.21)
>10 ¹⁶	5	1.29 (±0.12)
chlorine nitrate; i.r.		
4.1 × 10 ¹⁴	6 ^c	1.16 (±0.13)
9.5 × 10 ¹⁵	6 ^c	1.03 (±0.14)
1.31 × 10 ¹⁶	6 ^c	0.98 (±0.10)
chlorine dioxide		
10 ¹⁴ -<10 ¹⁵	7	1.00 (±0.09)
10 ¹⁵ -10 ¹⁶	7	1.08 (±0.26) ^d
>10 ¹⁶	3	0.95 (±0.1) ^d

^a $T = 303$ K, pressure 10-760 Torr. ^b σ' = one standard deviation. ^c Three successive measurements of both i.r. features indicated on fig. 3. ϕ according to eqn (iv). ^d Measured at 348 nm.

These experiments were conducted at a total pressure of 10 Torr, mainly N₂, and at room temperature (293 K).

Table 2 shows a summary of the yield measurements. They are grouped according to initial OClO concentration, since it was of interest to search for possible [OClO] dependence of the chemistry in view of the previous results of Molina *et al.*⁶ It will be seen that none of the average ϕ values given differ significantly from unity, with the possible exception of $\phi(\text{ClONO}_2)$ from eqn (ii) at high [OClO] which were significantly greater than unity. Although this is not reflected in the measured OClO loss rates for these conditions, which were apparently slightly lower than unity, measurement of OClO at 348 nm was not considered so reliable as at the band maximum (351.5 nm) owing to the lower absorption cross-section relative to possible interfering substances. Thus a slightly enhanced yield of ClONO₂ at high [OClO] cannot be ruled out, but the overall experimental uncertainty precludes a firm conclusion regarding such a small effect.

In the i.r. experiments, no systematic trends in the relative decay rates of ClONO₂ and OClO were evident, showing clearly that the stoichiometric equation according to reaction (10) applies for the photolysis of OClO-NO₂ mixtures over the whole range of [OClO] investigated:

**Rate Coefficients for the Reaction ClO + NO₂ + M → Products**

Rate coefficients were determined from time-resolved measurements of absorption due to ClO in the 11-0 band of the $A^2\Pi \leftarrow X^2\Pi$ transition at 277.2 nm. At the spectral slit width employed (0.27 nm), the band was fully resolved and the accepted⁴ value of $\sigma = 7.2 \times 10^{-18}$ cm² molecule⁻¹ was used to determine absolute ClO concentrations. In all experiments the concentration of NO₂ was in large excess over ClO, and ClO kinetics were pseudo-first-order, with the first-order rate constant defined by $k^1 = k_1[\text{NO}_2][\text{M}]$.

Fig. 6 shows a typical time profile of ClO during a single cycle of modulated photolysis of a flowing OClO-NO₂ mixture at 25 Torr. During illumination, [ClO] rises to a steady-

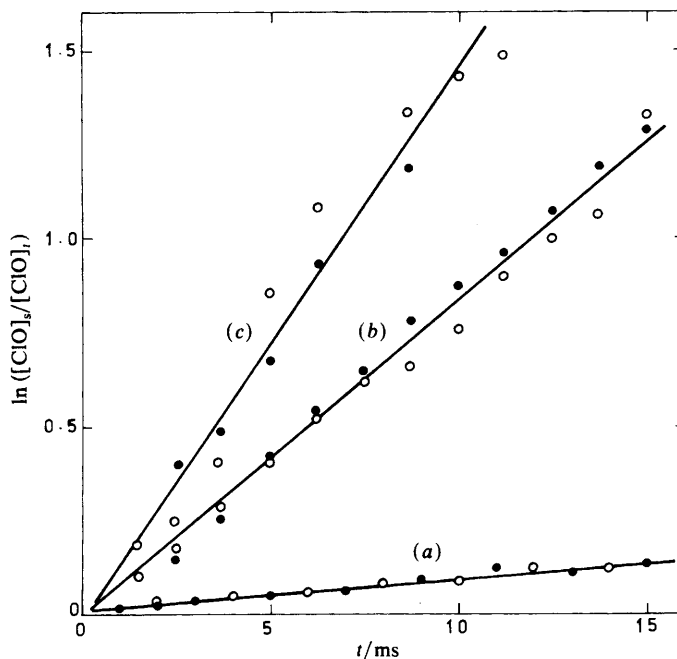


Fig. 7. Plots of $\ln([\text{ClO}]_s/[\text{ClO}]_t)$ vs. time for rise and fall of ClO to steady state ($[\text{ClO}]_s$) during the modulated photolysis of OClO-NO₂ mixtures. Filled points from rise to steady state during illumination. Open points from dark decay. $k^I = (a)$ 7.9, (b) 83.5 and (c) 145 s⁻¹.

state value according to the integrated form of the first-order rate equation:

$$[\text{ClO}]_t = \frac{B}{k^I} [1 - \exp(-k^I t)] \quad (\text{v})$$

where B is the rate of photolytic production of ClO. In the dark, ClO decays according to the equation

$$[\text{ClO}]_t = \frac{B}{k^I} \exp[-k^I(t - \tau/2)] \quad (\text{vi})$$

where τ is the photolysis period. Since the decay time is finite, a small residual concentration of ClO remains at the end of the cycle given by

$$[\text{ClO}] = \frac{B}{k^I} \left(\frac{1 - \exp(-k^I \tau/2)}{\exp(k^I \tau/2) - \exp(-k^I \tau/2)} \right) \quad (\text{v})$$

Approximate values of k^I were determined from the half-lives, $t_{0.5}$, for rise to and fall from steady state ($k^I \approx \ln 2/t_{0.5}$) and these were used together with σ and B to calculate residual absorption. The residual absorption was added to the observed and the first-order rate constants obtained by least-squares analysis of semilog plots. Some typical plots are shown in fig. 7. No significant departure from first-order behaviour could be detected over the entire range of reactant conditions used as judged from the linearity of the plots and the consistency of the k^I values from data for rise and fall to and from steady state.

Mean values of k^I from rise and fall were employed to determine k^{II} , the effective bimolecular rate coefficient ($k^I[\text{NO}_2]^{-1}$), using the average concentration of NO₂ present in the cell. $[\text{NO}_2]_{\text{av}}$ was calculated on the assumption of a linear concentration-gradient

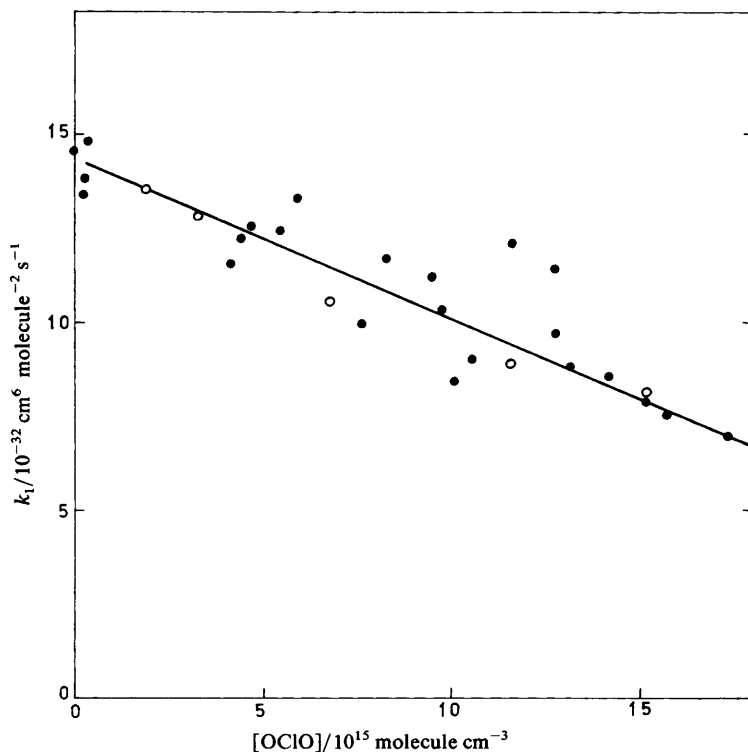


Fig. 8. Dependence of the rate coefficient k_1 on concentration of chlorine dioxide. Open points show data of Molina *et al.* [ref. (6)]. 26 Torr N₂, $T = 303$ K.

along the reaction cell, *i.e.*

$$[\text{NO}_2]_{\text{av}} = ([\text{NO}_2]_0 - B t_{\text{res}}) / 4 \quad (\text{vi})$$

where $B = 2k_a^{\text{OCIO}}[\text{OCIO}] + 2k_a^{\text{NO}_2}[\text{NO}_2]$ and t_{res} = residence time of the gas mixture in the cell. This assumption was justified since OCIO consumption was not more than *ca.* 8% and the contribution of NO₂ photolysis to the total NO₂ photolysis to the total NO₂ removal was only *ca.* 10%.

The majority of experiments were carried out at 25 ± 1 Torr and 303 K. Third-order rate constants for the association reaction were calculated from the k^{II} values. These are plotted on fig. 8 as a function of [OCIO] to facilitate comparison with the results obtained by Molina *et al.*⁶ using the flash-photolysis technique, which are indicated by the open points. The present work confirms the observations of Molina *et al.*⁶ of a definite decrease in the apparent value of k_1 with increasing OCIO. At low OCIO the value of $k_1 = (1.40 \pm 0.07) \times 10^{-31} \text{ cm}^6 \text{ molecule}^{-1} \text{ s}^{-1}$ is in excellent agreement with the value of $1.37 \times 10^{-31} \text{ cm}^6 \text{ molecule}^{-2} \text{ s}^{-1}$ obtained from the CODATA evaluation³ for 26 Torr total pressure. The values of k_1 fall off to *ca.* one-half of this value at 0.5 Torr [OCIO].

Considering that the magnitude of the decrease in k_1 over the considerable experimental range of reagent concentrations was only a factor of two, possible sources of error were examined. The experimental error on an individual determination of k_1 , taking into account uncertainties in the values of k^{I} , [NO₂] and total pressure, was *ca.* $\pm 20\%$. The decrease in k_1 is clearly significantly greater than can be accommodated by experimental error.

Potentially the most serious source of systematic error lies in the consumption of NO_2 during the course of the reaction along the monitoring path length for ClO, with a consequent decrease in the pseudo-first-order loss rate of ClO, k^I , along the cell. However, it can be shown that, providing $[\text{NO}_2]_{\text{av}}$ calculated from eqn (vi) is $\geq 75\%$ of the initial NO_2 concentration, *i.e.* not more than half of the NO_2 reactant is removed during passage through the cell, the value of k^{II} calculated from the expression $k^I([\text{NO}_2]_{\text{av}})^{-1}$ is less than 4% lower than the value obtained by full integration along the concentration gradient.¹⁷

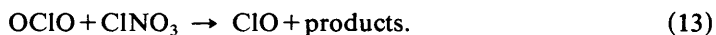
The experimental values of k_1 shown in fig. 8 were all obtained with NO_2 depletion of between 10 and 54% and therefore the maximum systematic error introduced in the data treatment was a *ca.* 5% underestimation of k_1 . The higher reagent consumption tended to be associated experiments with high [OCIO] since the amount of NO_2 present was limited by the maximum size of k^I that would be conveniently measured (*ca.* 200 s^{-1}). Nevertheless, the observed decline of a factor of two in k_1 could not be reasonably accounted for by systematic error arising from reagent depletion. Furthermore, a limited number of 'high' [OCIO] experiments with $<35\%$ depletion gave 'low' k_1 values.

Another possible source of systematic error in the ClO kinetics measurements is the presence of interfering absorption at the monitoring wavelength for ClO, 277.2 nm. As seen from table 1, NO_2 absorbs only weakly here, but OCIO absorption is stronger, although still considerably less than ClO. Since in a single modulated photolysis cycle the changes in concentration of reactants, products and transients are generally of the same magnitude, interference from the reactants should be minimal. In fact no evidence for strong characteristic product and reactant absorption near 277 nm was noted. The average value of the absorption cross-section for ClO at 277.2 nm calculated from analysis of the observed steady-state ClO absorptions ($= \sigma I B / k^I$) was $(7.7 \pm 1.0) \times 10^{-18} \text{ cm}^2 \text{ molecule}^{-1}$. This is in good agreement with the literature value and showed no systematic dependence on [OCIO].

It is therefore concluded that the apparent reduction in the first-order decay rate constants for ClO is a real kinetic effect associated with the presence of high concentrations of OCIO in the reaction mixtures.

Discussion

In the present work under conditions of high [OCIO], we have confirmed the observation first made by Molina *et al.*⁶ of an apparent decline of k_1 with increasing [OCIO]. Molina *et al.*⁶ have suggested that the decline in k_1 in their experiments could have been due to the reaction of OCIO with an isomeric product of the ClO- NO_2 reaction:



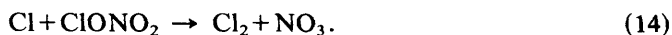
The measured overall rate constant for ClO decay at low [OCIO] (or in the presence of Cl_2O) is then due to both reactions (1) and (12). As [OCIO] increases, the rate of removal of ClO is reduced because the radical is regenerated in reaction (13), leading to an apparent fall in the rate constant for the reaction of ClO with NO_2 .

Isomer formation in the association reaction between ClO and NO_2 has also been proposed by Bhatia *et al.*¹⁸ based upon matrix-isolated *i.r.* spectra of samples of synthetic chlorine nitrate and products of the ClO- NO_2 reaction. Deposition of both samples from the gas phase gave spectral indications of the presence of at least one isomer, ClOONO, in addition to the stable form ClONO₂. The ClOONO species was relatively unstable and isomerized to the stable form upon warming the matrix to 40 K. The mechanism of formation of the ClOONO species in the cold matrix is, however, unclear.

Recently, Margitan¹⁹ reported work using 266 nm laser photolysis of known concentrations of chlorine nitrate and the equivalent amount of product from the ClO- NO_2

reaction, carried out in a discharge flow system. The similarity in the Cl atom yield from the two systems suggests that isomers other than ClONO₂ are not formed in the reaction of ClO with NO₂. The author also points out that the apparent discrepancy in the forward and reverse rates of reaction (1) discussed by Knauth⁵ can be attributed mainly to inadequate reliability of the value of ΔH_f° (ClONO₂) and hence of k_1^* based on thermochemical calculations.

A further important development in chlorine nitrate chemistry is the upward revision of the rate constant for the reaction



The most recently measured values of k_{14} ^{20,21} which are in good agreement are higher than the earlier accepted value by a factor of 50. This result has a profound effect in the interpretation of the data of Molina *et al.*⁶ for the OCIO–NO thermal reaction which was claimed to be supportive of the isomer theory. The low yields of ClONO₂ relative to NO₂ can now be qualitatively accounted for.¹⁹

Previous work in this laboratory⁸ found no evidence for the formation of any isomers as products of the reaction of ClO with NO₂ and this is confirmed by the ClONO₂ yields measured in the present work, where OCIO instead of Cl₂O has been used as a source of ClO. Our earlier results allowed an upper limit of 5 ms (298 K) to be established for the lifetime of any isomeric products, additional to ClONO₂ formed in reaction (1). The short lifetime of any isomer would require an unusually large rate constant for reaction (13) (considering that two non-radical species are involved) to explain the apparent decline in k_1 with increasing OCIO pressure.

One possible explanation for the observed decline in k_1 would involve storage of ClO as Cl₂O₃ or Cl₂O₂, formed in reactions (15) and (16), respectively,



followed by subsequent release by ClO by decomposition. This would serve to reduce the apparent decay rate of ClO due to reaction with NO₂. Molina *et al.*⁶ considered reaction (15), but they argued that it could not explain the observed decrease in k_1 under flash-photolysis conditions. The formation of Cl₂O₂ is not an attractive explanation since k_{16} is a factor of three slower than k_1 and [NO₂] in the present work was a factor of at least 100 higher than [ClO] at steady state. Thus, only a small fraction of the ClO could be stored and released through Cl₂O₂ on the time scale of a single photolysis cycle.

A further possible cause in the reduction in apparent reactivity of ClO with NO₂ at high [OCIO] is additional ClO production from the reaction



A possible source of Cl atoms is the reaction sequence



NO produced in reaction (18) could also lead to additional ClO production *via* reaction (4). The importance of reaction (18) would increase markedly with reagent concentration. Generation of additional ClO through these reactions would lead to an increased yield of ClONO₂ over that expected from the photochemical reaction. The experimental results indeed show that this may be the case at high [OCIO]. A value of k_{18} of the order of 10⁻¹⁸ cm³ molecule⁻¹ s⁻¹ would be required to explain the apparent 30% increase in ClONO₂ yield.

The occurrence of reaction (18) could also lead to complications because the product ClO₃ exhibits strong absorption throughout the near and middle u.v. and could potentially

interfere with absorption measurements (e.g. those for OCIO at 348 nm). The presence of a thermal source of ClO would also lead to an overestimation of $[\text{NO}_2]_{\text{av}}$ as calculated from eqn (vi), thereby leading to an underestimation of k_1 . This effect would be in addition to any apparent kinetic effect on ClO decay resulting from the additional radical source. Clearly the determination of k_1 in this system is sensitive to the presence of non-photochemical CClO production from the precursor, OCIO.

The measured rate constant for k_1 at 26 Torr total pressure and 303 K under conditions of low $[\text{OCIO}]$ ($<10^{15}$ molecule cm^{-3}) was in excellent agreement with the agreed value from the CODATA evaluation.³ A very recent paper from Handwerk and Zellner²² has confirmed that k_1 is in the third-order region at 25 Torr pressure and that fall-off begins only at pressures above 50 Torr. The product yield measurements in the present study confirm that the recommended rate constant for the ClO-NO₂ reaction refers to ClONO₂ formation and is the correct value to use to evaluate the stratospheric ClONO₂ formation rate.

This work was sponsored by the Chemical Manufacturers Association project number FC-82-400. T.J.W. acknowledges the support of an S.E.R.C. CASE award. We thank Dr Mario J. Molina and Dr James J. Margitan for helpful discussions.

References

- 1 *The Stratosphere—Present and Future*, ed. R. D. Hudson and E. I. Reed (NASA Reference Publication 1049, 1979), p. 333.
- 2 F. S. Rowland, J. E. Spencer and M. J. Molina, *J. Phys. Chem.*, 1976, **80**, 2711.
- 3 D. L. Baulch, R. A. Cox, P. J. Crutzen, R. F. Hampson Jr., J. A. Kerr, J. Troe and R. T. Watson, *J. Phys. Chem. Ref. Data*, 1982, **11**, 327.
- 4 NASA Panel for Data Evaluation, *Chemical Kinetics and Photochemical Data for Use in Stratospheric Modelling*, W. B. DeMore, M. J. Molina, R. T. Watson, D. M. Golden, R. F. Hampson, M. J. Kuryto, C. J. Howard and A. R. Revishankara (J.P.L. Publication 83-62, 1983), p. 83.
- 5 H. D. Knauth, *Ber. Bunsenges. Phys. Chem.*, 1978, **82**, 212.
- 6 M. J. Molina, L. T. Molina and T. Ishiwata, *J. Phys. Chem.*, 1980, **84**, 3100.
- 7 J. S. Chang, A. C. Baldwin and D. M. Golden, *J. Chem. Phys.*, 1979, **71**, 2021.
- 8 R. A. Cox, J. P. Burrows and G. B. Coker, *Int. J. Chem. Kinet.*, in press.
- 9 R. A. Cox, D. W. Sheppard and M. P. Stevens, *J. Photochem.*, 1982, **19**, 189.
- 10 M. Schmeisser, *Inorg. Synth.*, 1967, **9**, 127.
- 11 G. H. Gady, *Inorg. Synth.*, 1957, **5**, 156.
- 12 J. A. Davidson, A. A. Viggiano, C. J. Howard, I. Dotan, F. C. Fehsenfeld, D. L. Albritton and E. E. Ferguson, *J. Chem. Phys.*, 1978, **65**, 2085.
- 13 L. S. Rothman, A. Goldman, J. R. Gillis, R. H. Tipping, L. R. Brown, J. S. Margolis, A. G. Maki and L. D. G. Young, *Appl. Opt.*, 1980, **20**, 1323.
- 14 H. Niki, P. D. Maker, C. M. Savage and L. P. Breitenbach, *Chem. Phys. Lett.*, 1978, **59**, 78.
- 15 D. E. Tevault and R. R. Smardzewski, *J. Chem. Phys.*, 1979, **67**, 3777.
- 16 D. L. Bernitt, R. H. Miller and I. C. Hisatsune, *Spectrochim. Acta, Part A*, 1967, **23**, 237.
- 17 R. A. Cox and R. Lewis, *J. Chem. Soc., Faraday Trans. 1*, 1979, **75**, 2649.
- 18 S. C. Bhatia, M. George-Taylor, C. W. Meredith and J. W. Hall Jr, *J. Phys. Chem.*, 1983, **87**, 1091.
- 19 J. J. Margitan, *J. Geophys. Res.*, 1983, **88**, 5416.
- 20 J. J. Margitan, *J. Phys. Chem.*, 1983, **87**, 674.
- 21 M. J. Kurylo, G. L. Knoble and J. L. Murphy, *Chem. Phys. Lett.*, 1983, **95**, 9.
- 22 V. Handwerk and R. Zellner, *Ber. Bunsenges. Phys. Chem.*, 1984, **88**, 405.